# *Force analysis of an under actuated robotic finger*

Dr R.Vivekananthan, Asst. prof., Department of Mechanical Engineering, Government college of Engineering,Salem-11
rvivekapme@gmail.com
K.Ranjithkumar, PG scholar, Department of Mechanical Engineering& Government college of Engineering,Salem-11
ranjithkumar0211@gmail.com

A.Mozhialagan*, PG scholar, Department of Mechanical Engineering& Government college of Engineering,Salem-11
mozhialagan0307@gmail.com

***Abstract*—Commercially available under actuated robotic finger are often expensive and difficult to modify. But this kind of under actuated finger is small size and light weight. The finger possess self-adaptive grasping the object depending on grasping force. The development of mathematical model to calculate the torque. Thus, the mathematical calculation is used for evaluating finger parameters in noncontact link position. The dynamic model of the linkages is integrated with the hydraulic actuator. The experimental process is to obtain the contact force between the gripper and object using LABVIEW software. In this experiment, the grasping force is measured and compared with mathematical results.**

***Keywords*-*graspingforce,labview,robotic finger,phalanx.***

## INTRODUCTION

Compact Under actuated robotic hand plays a vital role in the prosthetics application. The amputees who lost their arms due to accidents wear prosthetic hands and use these instruments to facilitate them in performing their daily activities. Besides that, this type of hand is also significant in the humanoid field, where the robots are required to carry out tasks in the same working environment as human beings and are expected to achieve high performance and capability as human. These hands are developed to either or both serve the functions of a real hand and mimic its physical appearance. This is due to the fact that there are not many components including the motors and reduction gears that are small and light enough to realize practical hand movements [1]. Some of the previous hands including the UTAH/ MITH and [2] and Stanford/ JPL Hand [3] achieve good performances in replicating human capabilities, but are bulky and heavy due to the large size and number of actuators and sensors incorporated. The RTRII Hand [4] and SARAHHAND [5-7] possess compact designs with high degree of freedom (DOF) by adopting the under-actuated mechanism.

In this design, the commonly used active motors are replaced by small passive elements such as springs and mechanical limits. However, these fingers can only grasp objects with its self-adaptive grasping capability. The robotic gripper configuration gives maximum configuration range and minimum contact force for a wide range of target object sizes and position [8].

The design is to develop a mechanism that can realize the same shape, size and weight but operates and moves similar to a human hand. Some examples of previous hands with high functionality but bulky and heavy due to the number of sensors incorporated include [9] and [10]. The fingers in [11] and [12] are light in weight and small in size, which are close to a human hand physical appearance, but they are limited to grasping functions only. The mathematical model of the whole finger is developed based on the four bar mechanism model in [13].

From the above discussion, it can be understood that each type of grippers has its advantages and disadvantages. In this paper, investigate the dynamic behavior of a anthropomorphic finger mechanism that is able to perform self-adaptive grasping operations.

## ROBOTIC FINGER MECHANISM

The robotic finger possesses a lighter weight and closer size to human finger whilst able to provide the sufficient force required to accomplish grasping tasks. There is no gear transmission within the phalanges. The under actuated robotic finger consist of proximal, middle and distal phalanxes. The finger is driven by hydraulic actuator and drive input force is calculated. when the input torque is applied on link2, the finger rotates around joint 1 until the proximal phalanxes touches the object. The proximal phalanx will stop to move after being in contact with the object. Next, further transmission mechanism will cause the middle and distal phalanx to rotate until the finger has wrapped the object. In this setup, sensors are mounted to measure the forces of each phalanx and these sensors interface with computer.

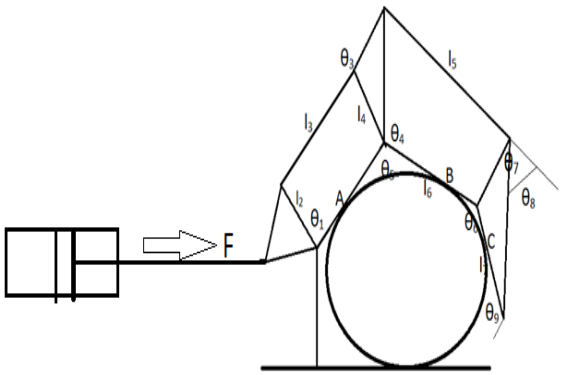


**Fig. 1** Grasping sequence of circular object

The finger mechanism is composed of two four-bar linkages connected in series and the distal phalanx at the end. When apply the input force to first four bar mechanism and the output is taken from all the contact links. In this three links are formed to three different angles of the gripper to grasp the object.

## DYNAMIC MODEL OF MECHANICAL LINKAGES

Fig 2 represents the under actuated robotic finger. The finger operate in horizontal plane, therefore the potential energy is neglected due to the gravitational effect. It is also assumed that the model is made for the finger is not contact with any object.

From the legrange's equation, the mathematical model of the robotic system is

$$\frac{d}{dt}\left(\frac{\partial K}{\partial \dot{\theta}_j}\right)-\frac{\partial K}{\partial \theta_j}+\frac{\partial P_o}{\partial \theta_j}=T_j$$

Where

*K* is the kinetic energy,

*Po* is the potential energy of the system,

*T* is the generalized torque,

*j* denotes the generalized coordinates.

The kinetic energy of the system, *K* can be expressed as

$$K=\sum_{i=2}^{7}\left(\frac{1}{2}m_i\left(V_{ix}^2+V_{iy}^2\right)+\frac{1}{2}J_i\dot{\theta}_i^2\right)$$

Where

$\theta_i$is the angular velocity of link *i*,

$V_{ix}$ and $V_{iy}$ are the *x* and *y* axis velocity components

The chain product of partial differentiation with respect to $\Theta_2$ as

$$V_{ix}=\frac{\partial X_{ci}}{\partial \theta_2}\frac{d\theta_2}{dt}$$

$$V_{iy}=\frac{\partial Y_{ci}}{\partial \theta_2}\frac{d\theta_2}{dt}$$

$$\dot{\theta}_i=\frac{\partial \theta_i}{\partial \theta_2}\frac{d\theta_2}{dt}$$

Therefore K can rewritten as

$$K=\frac{1}{2}\dot{\theta}_2^2\sum_{i=2}^{7}\left(m_i\left(\left(\frac{\partial X_{ci}}{\partial \theta_2}\right)^2+\left(\frac{\partial Y_{ci}}{\partial \theta_2}\right)^2\right)+J_i\left(\frac{\partial \theta_i}{\partial \theta_2}\right)^2\right)$$

and can be simplified as

$$K=\frac{1}{2}\dot{\theta}_2^2 A$$

Where

$$A=\sum_{i=2}^{7}\left(m_i\left(\left(\frac{\partial X_{ci}}{\partial \theta_2}\right)^2+\left(\frac{\partial Y_{ci}}{\partial \theta_2}\right)^2\right)+J_i\left(\frac{\partial \theta_i}{\partial \theta_2}\right)^2\right)$$

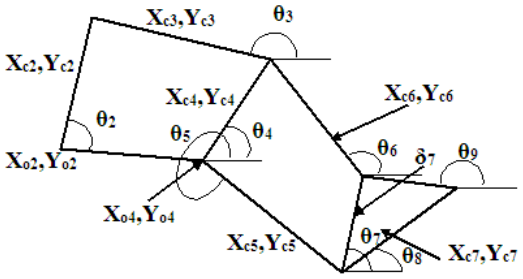


**Fig. 2** Finger configuration

| Notation | Parameter |
|---|---|
| $\theta_i$ | angular displacement of *i*th link |
| $\dot{\theta}_i$ | angular velocity of *i*th link |
| $\ddot{\theta}_i$ | angular acceleration of *i*th link |
| $m_i$ | mass of *i*th link |
| $j_i$ | moment of inertia of *i*th link |
| $l_i$ | length of *i*th link |
| $r_i$ | mass centre of *i*th link |

**Table 1** Linkage parameter notation

Substituting$\left(\frac{\partial X_{ci}}{\partial \theta_2}\right)^2+\left(\frac{\partial Y_{ci}}{\partial \theta_2}\right)^2$ and $\frac{\partial \theta_i}{\partial \theta_2}$expressions as in APPENDIX and simplifying the equation, A becomes

$$A=C_1+C_2\left(\frac{\partial\theta_3}{\partial\theta_2}\right)^2+(C_3+C_5)\left(\frac{\partial\theta_4}{\partial\theta_2}\right)^2+C_4 \frac{\partial\theta_3}{\partial\theta_2}cos(\theta_3-\theta_2)+ \left(\frac{\partial\theta_4}{\partial\theta_2}\right)^2\left[C_6\left(\frac{\partial\theta_6}{\partial\theta_4}\right)^2+ C_7\left(\frac{\partial\theta_7}{\partial\theta_4}\right)^2+C_8\frac{\partial\theta_6}{\partial\theta_4}cos(\theta_6-\theta_4)+C_9\frac{\partial\theta_7}{\partial\theta_4}cos(\theta_7-\theta_5)\right]$$

**Table 2** Geometric parameters of the linkages

| Length of the link in cm | | Degree | |
|---|---|---|---|
| $l_2$ | 12 | $\theta_2$ | 65 |
| $l_3$ | 16 | $\theta_3$ | 160 |
| $l_4$ | 7.5 | $\theta_4$ | 60 |
| $l_5$ | 16.5 | $\theta_5$ | 320 |
| $l_6$ | 13.5 | $\theta_6$ | 140 |
| $l_7$ | 11 | $\theta_7$ | 120 |

The assumption that the robotic finger operates in horizontal plane the torque due to the linkages can be described by

$$T = A\ddot{\theta}_2 + \frac{1}{2}\frac{dA}{d\theta_2}\dot{\theta}_2^2$$

$=1350.91*0.992+½ * -159.39*(1.5)^2$

$=11.60$ Nm

Input force

$F_2=11.60/0.12$

$=96.66$N

## EXPERIMENTAL PROCESS

In this experiment, contact force is measured for an under actuated robotic finger. For measuring the contact force, tactile force sensor is used. The sensor measures force range upto 210N. The object can be made contact with this sensor. The contact sensor are pasted into the phalanges plane to measure the contact force.

**Fig. 3** Experimental setup

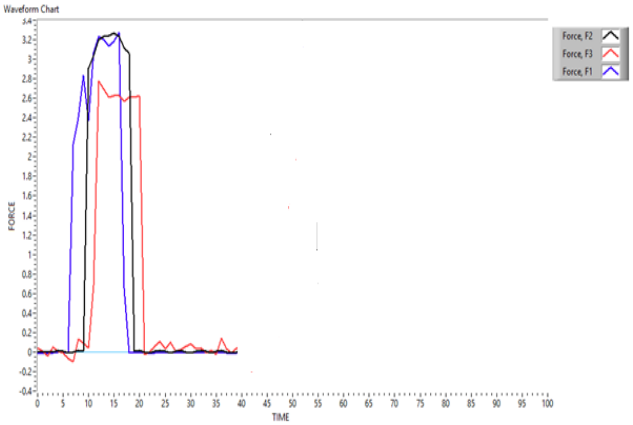


**Fig. 4** Contact forces

The contact forces of the links obtained from the contact sensors are

F1 = 32.34N

F2 = 31.36N

F3 = 25.48N

The sensors are interfaced with data acquisition system through lab view software for measuring contact forces. In this experiment, the grasping force is measured and

tabulated the grasping force value. This total contact force on the object is compared with input force at link 2.

## RESULTS AND DISCUSSION

In this paper, the total contact force on the under actuated robotic finger was calculated and the applied input force to be calculated by design parameters such as link length and angles. In this mathematical model, the calculated force value is 96.66 N.

From the experiment, the total grasping force to be measured was 89.27N. From the results the total contact force on the object is relative to the input force applied. The gripper design is varied by the dimension and distribution of the applied force to the phalanges affect the performance.

The total contact forces of the sensors is measured and compared the results. The total contact force is calculated by sum of the three forces obtained from sensors. From the results, it concludes that the finger is in closed condition, the input force and contact force of the object approximately equal.

The under actuated robotic finger was grasping the object, proximal phalanx of the finger maintain high contact force and then other two phalanx likely due to more contact force.

## CONCLUSION

The mathematical and experimental study on force analysis of a compact robotic finger is presented in this paper. The mathematical model is to calculate input force using linkage parameters and obtained the contact force for the under actuated robotic finger experimentally. The relation of the input force and the contact force on the object is found approximately linear. The calculated resultant forces are verified by conducting an experiment which influence good grasping ability.

## REFERENCE


1.K.Hoshino,I.Kawabuchi, "Dexterous Robot Hand with Pinching Function at Fingertips", in 2006 IEEE/RAS-EMBS International Conference on Biomedical Robotics and Biomechatronics, pp. 1113-1118

2.S. G. Jacobsen, E. K. Iversen, D. F. Knutti, R. T. Johnson, K. B. Biggers, "Design of the Utah/M.I.T. Dextrous Hand", in 1986 IEEE International Conference on Robotics and Automation, pp.1520-1532

3.M. T. Mason, J. K. Salisbury, Robot Hands and the Mechanics of Manipulation. USA: MIT Press, 1985

4.B. Massa, S. Rocella, M. C. Carozza and P. Dario, "Design and Development of an Underactuated Prosthetic Hand", in 2002 IEEE International Conference on Robotics and Automation, pp. 3374-3379

5.T. Laliberte and C. M. Gosselin, "Underactuation in Space Robotic Hands", in 2001International Symposium on Artificial Intelligence and Robotics & Automation in Space, pp. 1-8.

6.T. Laliberte, L. Birglen and C. M. Gosselin, "Underactuation in robotic grasping hands", Machine Intelligence &Robotic Control, vol. 4, no. 3, pp. 1-11, 2002

7.S. G. Jacobsen, E. K. Iversen, D. F. Knutti, R. T. Johnson, K. B. Biggers, "Design of the SARAHDextrous Hand", in 1986 IEEE International Conference on Robotics and Automation, pp.1520-1532
8.Yoshikawa.T and Nagai.K, ' Manipulating and grasping forces in manipulation by multifingered robot hands', IEEE Transactions on Robotics, vol.7, issue 1, 2002, 67-77.
9.S. G. Jacobsen, E. K. Iversen, D. F. Knutti, R. T. Johnson, K. B. Biggers, "Design of the Utah/M.I.T. Dextrous Hand", in 1986 IEEE International Conference on Robotics and Automation, pp.1520-1532.
10. M. T. Mason, J. K. Salisbury, Robot Hands and the Mechanics of Manipulation. USA: MIT Press, 1985.
11. B. Massa, S. Rocella, M. C. Carozza and P. Dario, "Design and Development of an Underactuated Prosthetic Hand", in 2002 IEEE International Conference on Robotics and Automation, pp. 3374-3379.
12. N. Fukaya, S. Toyama , T. Asfour and R. Dillmann, "Design of the TUAT/ Karlsruhe Humanoid Hand", in the Proceedings of the 2000 IEEE/RSJ International Conference on Intelligent Robots and Systems, 2000, pp. 1754- 1759
13.J. Tao and J. P. Sadler, "Constant Speed Control of a Motor Driven Mechanism System", Mechanism and Machine Theory, vol 30, pp737-748, 1994

## APPENDIX

$$C_1 = m_2 r_2^2 + J_2 + m_3 l_2^2$$

$$C_2 = m_3 r_3^2 + J_3$$

$$C_3 = m_4 r_4^2 + J_4$$

$$C_4 = 2 m_3 l_2 r_3$$

$$C_5 = m_5 r_5^2 + J_5$$

$$C_6 = m_6 r_6^2 + J_6$$

$$C_7 = m_7 r_7^2 + J_7$$

$$C_8 = 2 m_6 l_4 r_6$$

$$C_9 = 2 m_7 l_5 r_7$$

$$\frac{\partial \theta_3}{\partial \theta_2} = -\frac{l_2 \sin(\theta_2 - \theta_4)}{l_3 \sin(\theta_3 - \theta_4)}$$

$$\frac{\partial \theta_4}{\partial \theta_2} = -\frac{l_2 \sin(\theta_2 - \theta_3)}{l_4 \sin(\theta_3 - \theta_4)}$$

$$\frac{\partial \theta_6}{\partial \theta_4} = \frac{-l_4 \sin(\theta_4 - \theta_7) + l_5 \sin(\theta_5 - \theta_7)}{l_6 \sin(\theta_6 - \theta_7)}$$

$$\frac{\partial \theta_7}{\partial \theta_4} = \frac{-l_4 \sin(\theta_4 - \theta_6) + l_5 \sin(\theta_5 - \theta_6)}{l_7 \sin(\theta_6 - \theta_7)}$$

$$\frac{dA}{d\theta_2} = 2C_2 \frac{\partial\theta_3}{\partial\theta_2}\left(\frac{\partial^2\theta_3}{\partial\theta_2^2}\right) + 2(C_3 + C_5)\left(\frac{\partial\theta_4}{\partial\theta_2}\right)\left(\frac{\partial^2\theta_4}{\partial\theta_2^2}\right) + C_4\left[\frac{\partial^2\theta_3}{\partial\theta_2^2}\cos(\theta_3 - \theta_2) - \frac{\partial\theta_3}{\partial\theta_2}\sin(\theta_3 - \theta_2)\left(\frac{\partial\theta_3}{\partial\theta_2} - 1\right)\right] + 2\left(\frac{\partial\theta_4}{\partial\theta_2}\right)\left(\frac{\partial^2\theta_4}{\partial\theta_2^2}\right)\left[C_6\left(\frac{\partial\theta_6}{\partial\theta_4}\right)^2 + C_7\left(\frac{\partial\theta_7}{\partial\theta_4}\right)^2 + C_8\frac{\partial\theta_6}{\partial\theta_4}\cos(\theta_6 - \theta_4) + C_9\frac{\partial\theta_7}{\partial\theta_4}\cos(\theta_7 - \theta_5)\right] + \left(\frac{\partial\theta_4}{\partial\theta_2}\right)^2\left\{2C_6\left(\frac{\partial\theta_6}{\partial\theta_4}\right)\left(\frac{\partial^2\theta_6}{\partial\theta_4^2}\right) + 2C_7\left(\frac{\partial\theta_7}{\partial\theta_4}\right)\left(\frac{\partial^2\theta_7}{\partial\theta_4^2}\right) + C_8\left[\frac{\partial^2\theta_6}{\partial\theta_4^2}\cos(\theta_6 - \theta_4) - \frac{\partial\theta_6}{\partial\theta_4}\sin(\theta_6 - \theta_4)\left(\frac{\partial\theta_6}{\partial\theta_4} - 1\right)\right] + C_9\left[\frac{\partial^2\theta_7}{\partial\theta_4^2}\cos(\theta_7 - \theta_4) - \frac{\partial\theta_7}{\partial\theta_4}\sin(\theta_7 - \theta_4)\left(\frac{\partial\theta_7}{\partial\theta_4} - 1\right)\right]\right\}$$